

# $\Lambda$ CDM without cosmological constant

L. N. Granda\*

*Departamento de Fisica, Universidad del Valle*

*A.A. 25360, Cali, Colombia*

## Abstract

The introduction of a kind of exponential damping in the correction to General Relativity gives promising results in the construction of viable dark energy model in the context of modified gravity. The model behaves as  $R - 2\Lambda$  at large curvature and tends to zero at  $R \rightarrow 0$ , containing flat spacetime solution and implying that the curvature effect that induces the accelerated expansion is unrelated to quantum vacuum energy in flat space-time. The cosmic evolution of the main density parameters in this model is consistent with current observations with an equation of state very close to  $-1$  and the effective equation of state showing the transition deceleration-acceleration at  $z \sim 0.5$ . Apart from viable cosmology, satisfying cosmological and local gravity restrictions, the model may also show measurable differences with  $\Lambda$ CDM at recent times. Some features of the present model that highlight differences with the Hu-Sawicki model are discussed.

## 1 Introduction

Modified gravity models have gained interest with the recent discovery of the gravitational waves that also imposed stringent restriction on the velocity of its propagation. Due to this restriction, some dark energy scalar-tensor models and models belonging

---

\*luis.granda@correounivalle.edu.co

to the class of Horndeski or Galilean theories [1, 2, 3] have been severely restricted, to the point of being discarded. Though the modified gravity models can avoid the restriction imposed by the velocity of gravitational waves, they have to pass severe restrictions mostly related with the local gravity tests. At cosmological scales they must be very close to, currently most successful dark energy model,  $\Lambda$ CDM (for review see [4, 5, 6, 7]) but locally they must reproduce with great accuracy the results of General Relativity. The function  $f(R)$  that generalizes the Einstein-Hilbert Lagrangian must contain corrections that are non-linear functions of the curvature (see [8, 9, 10, 11, 12, 13] for reviews).

These corrections should play an important role in the late universe and provide the necessary conditions for the transition from the decelerated to the accelerated phase of expansion, consistent with current observations, and at the same time these corrections should not be significant for local gravitational systems. Among the variety of proposed models that cause accelerated expansion are [8, 14, 15, 16, 17, 18, 19, 20, 21, 22, 23, 24, 25, 26, 27, 28, 29, 30, 31, 32, 33, 34, 35, 36, 37, 38, 39, 40, 41, 42, 43, 44, 45, 46, 47, 48, 49]. Models containing positive and negative powers of curvature are among the first and most studied corrections to the Einstein-Hilbert Lagrangian, where it was found that corrections with positive powers of curvature are relevant at early times, like in the case of  $R^2$  Starobinsky model [50], while models with negative powers of curvature, which although lead to late time accelerating universe, contain instabilities that prevent them from having a matter dominated era [51, 52, 17, 33] and are also inconsistent with solar system tests. Attempts to unify early time inflation with late time acceleration have been considered in [17, 53, 54, 55]. The Gauss-Bonnet 4-dimensional invariant has also been considered in the context of modified gravity in [56, 57, 58, 59], where it was shown that some functions of the Gauss-Bonnet invariant can lead to viable cosmological solutions with accelerated expansion. Exact cosmological solutions have been studied in [60, 61, 62, 63, 64, 65, 66] and  $f(R)$  models that can satisfy both cosmological and local gravity constraints have been proposed in [44, 67, 68, 69, 70, 71]. Cosmological scenarios resulting from various models of modified gravity have been investigated using the dynamical systems approach, which allows to find the critical points of the models that describe

the different phases of evolution of the universe [40, 45, 72, 10, 73, 74, 75, 76].

Despite the large number of works devoted to explaining late time the accelerated expansion of the universe, the definitive answer to the dark energy problem is still lacking. Modified gravity models face many challenges related to having to satisfy simultaneously large scale cosmological restrictions and stability conditions while being practically indistinguishable from General Relativity at local gravity scales. Thus, most models that may be cosmologically viable produce distortions in the metric at the level of the solar system leading to inconsistencies with observations. To satisfy solar-system constraints some models give rise to the chameleon mechanism that arises when the curvature of a local system is very large compared to background curvature [44, 77, 78].

In the present paper we continue the study of modified gravity with an exponential function of the curvature [79, 80], where anew parameter is introduced that leads to a richer variety of viable cosmological scenarios. The model is able to account for all above discussed restrictions, apart from the stability conditions and very accurate description of the dark energy according to current observations. At large curvature the model behaves as  $f(R) = R - 2\Lambda$  and  $f(R \rightarrow 0) = 0$  allowing Minkowski flat spacetime solution. So the curvature effect that induces the accelerated expansion is unrelated to quantum vacuum energy in flat space-time. It is shown that the condition of stability ( $f''(R) > 0$ ) takes place during the whole cosmological evolution and even beyond the de Sitter phase.

This paper is organized as follows. In section 2 we present the general features of the  $f(R)$  models, including the dynamical system and the relevant critical points for our study in terms of the  $(r, m)$  parameters. In section 3 we present the models, showing the conditions for stability and viability and some numerical study comparing it with the Hu-Sawicki model. Some discussion is given in section 4.

## 2 Field equations and constraints for $f(R)$

The modified gravity is described by a general action of the form

$$S = \int d^4x \sqrt{-g} \left[ \frac{1}{2\kappa^2} f(R) + \mathcal{L}_m \right] \quad (2.1)$$

where  $\kappa^2 = 8\pi G$ ,  $f(R)$  is a function of curvature that contains the linear Einstein term and non-linear corrections to it, and  $\mathcal{L}_m$  is the Lagrangian density for the matter component which satisfies the usual conservation equation. Variation with respect to the metric gives the equation of motion

$$f_{,R}(R)R_{\mu\nu} - \frac{1}{2}g_{\mu\nu}f(R) + (g_{\mu\nu}\square - \nabla_\mu\nabla_\nu) f_{,R}(R) = \kappa^2 T_{\mu\nu}^{(m)} \quad (2.2)$$

where  $T_{\mu\nu}^{(m)}$  is the matter energy-momentum tensor and  $f_{,R} \equiv \frac{df}{dR}$ . The trace of eq. (2.2) gives

$$Rf_{,R}(R) - 2f(R) + 3\square f_{,R}(R) = \kappa^2 T^{(m)} = \kappa^2 (3p - \rho) \quad (2.3)$$

The time and spatial components of the Eq. (2.2) are given by the following expressions

$$3H^2 f_{,R} = \frac{1}{2} (Rf_{,R} - f) - 3H\dot{f}_{,R} + \kappa^2 \rho \quad (2.4)$$

and

$$-2\dot{H}f_{,R} = \ddot{f}_{,R} - H\dot{f}_{,R} + \kappa^2(\rho + p) \quad (2.5)$$

where dot represents derivative with respect to cosmic time. The field equation (2.4) can be written in more compact form by defining the effective energy density as follows

$$H^2 = \frac{\kappa^2}{3} \rho_{eff}, \quad (2.6)$$

where

$$\rho_{eff} = \frac{1}{f_{,R}} \left[ \frac{1}{2\kappa^2} (Rf_{,R} - f - 6H\dot{f}_{,R}) + \rho \right] \quad (2.7)$$

The Eqs. (2.4) and (2.5) lead to the following effective equation of state (EoS)

$$w_{eff} = -1 - \frac{2\dot{H}}{3H^2} = -1 + \frac{\ddot{f}_{,R} - H\dot{f}_{,R} + \kappa^2(\rho + p)}{\frac{1}{2}(Rf_{,R} - f) - 3H\dot{f}_{,R} + \kappa^2\rho}, \quad (2.8)$$

where  $\rho$  and  $p$  include both matter and radiation components, i.e.  $\rho = \rho_m + \rho_r$  and  $p = p_m + p_r$ .

### Stability and Cosmological Constraints.

The first type of constraints that a modified gravity model  $f(R)$  must obey are related with the stability and the avoidance of unwanted ghosts or tachyonic degrees of freedom. The condition  $f_{,R} > 0$  for all  $R$  is necessary to avoid changing the sign of the effective Newtonian coupling (preserving the nature of the graviton) preventing ghosts instabilities. The condition  $f_{,RR} > 0$  is required for the stability under matter perturbations at high curvature regime. In fact the scalar particle associated with  $f(R)$ , dubbed scalaron with mass (in matter epoch or in the regime  $M^2 \gg R$ )

$$M^2 \simeq \frac{1}{3f_{,RR}}, \quad (2.9)$$

requires  $f_{,RR} > 0$  in order to avoid tachyonic behavior.

A second type of constraints is related with cosmological viability, and for this analysis it is useful to consider the dynamical system for the model (2.1) in order to find the cosmological scenarios arising from the critical points and its stability properties. To this end we use the following dimensionless variables [40, 45, 10], that reduce the Eq. (2.4) to a dynamical constraint (in what follows we will use indistinctly  $f_{,R}$  or  $F = f_{,R}$ )

$$x = -\frac{\dot{F}}{HF}, \quad y = -\frac{f}{6H^2F}, \quad z = \frac{R}{6H^2} = \frac{\dot{H}}{H^2} + 2, \quad w = \frac{\kappa^2 \rho_r}{3H^2F}, \quad \Omega_m = \frac{\kappa^2 \rho_m}{3H^2F} \quad (2.10)$$

which lead to the following dynamical system

$$x + y + z + w + \Omega_m = 1 \quad (2.11)$$

$$\frac{dx}{dN} = x^2 - xz - 3y - z + w - 1 \quad (2.12)$$

$$\frac{dy}{dN} = xy + \frac{xz}{m} - 2y(z - 2) \quad (2.13)$$

$$\frac{dz}{dN} = -\frac{xz}{m} - 2z(z - 2) \quad (2.14)$$

$$\frac{dw}{dN} = xw - 2zw \quad (2.15)$$

where  $N = \ln a$ ,  $w = \Omega_r$  is the density parameter of the radiation component, and  $m$  is given by

$$m = \frac{Rf_{,RR}}{f_{,R}}. \quad (2.16)$$

Along with the parameter  $m$  there is another useful parameter  $r$  defined as

$$r = -\frac{Rf_{,R}}{f}. \quad (2.17)$$

These parameters are useful to analyze the cosmological viability of  $f(R)$  models and characterize the deviation of a given  $f(R)$  model from the standard  $\Lambda$ CDM model, which corresponds to the line  $m = 0$ . In terms of these variables the effective EoS (2.8) can be written as

$$w_{eff} = -\frac{1}{3}(2z - 1), \quad (2.18)$$

while the dark energy equation of state from (2.4) and (2.5) can be written as

$$w_{DE} = -\frac{1}{3} \frac{2z - 1 + (F/F_0)w}{1 - (F/F_0)(1 - x - y - z)}, \quad (2.19)$$

where  $F_0$  is the current value of  $f_{,R}$ .

Among the critical points of the above system we will consider three of special interest for viable cosmological scenarios related to our model (see [40, 45, 10] for complete description).

The first critical point gives rise to scaling solutions including the matter dominated era is given by (in absence of radiation ( $w = 0$ ))

$$P_S = (x_c, y_c, z_c) = \left( \frac{3m}{1+m}, -\frac{1+4m}{2(1+m)^2}, \frac{1+4m}{2(1+m)} \right), \quad (2.20)$$

which gives the following matter density parameter and effective EoS

$$\Omega_m = 1 - \frac{m(7+10m)}{2(1+m)^2}, \quad w_{eff} = -\frac{m}{1+m}, \quad (2.21)$$

with eigenvalues

$$EV(P_S) : \left( 3(1+m'), \frac{-3m \pm \sqrt{m(256m^3 + 160m^2 - 31m - 16)}}{4m(m+1)} \right), \quad (2.22)$$

where prime represents derivative with respect to  $r$ .

The second critical point is a de Sitter attractor

$$P_{deS} = (x_c, y_c, z_c) = (0, -1, 2), \quad \Omega_m = 0, \quad w_{eff} = -1 \quad (2.23)$$

with eigenvalues

$$EV(P_{deS}) : \left( -3, -\frac{3}{2} \pm \frac{\sqrt{25 - 16/m(r = -2)}}{2} \right), \quad (2.24)$$

The third critical point that leads to accelerated solutions is

$$P_C = (x_c, y_c, z_c) = \left( \frac{2(1-m)}{1+2m}, \frac{1-4m}{m(1+2m)}, -\frac{(1-4m)(1+m)}{m(1+2m)} \right), \quad (2.25)$$

with the main parameters

$$\Omega_m = 0, \quad w_{eff} = \frac{2 - 5m - 6m^2}{3m(1+2m)}, \quad (2.26)$$

and the corresponding eigenvalues

$$EV(P_C) : \left( -4 + \frac{1}{m}, \frac{2 - 3m - 8m^2}{m(1+2m)}, -\frac{2(m^2 - 1)(1+m')}{m(1+2m)} \right). \quad (2.27)$$

From the coordinates  $y$  and  $z$  for the points  $P_S$  and  $P_C$  it can be seen that they are connected by the line  $m(r) = -1 - r$ , where the relation  $r = z/y$  is used.

From (2.20) follows that the matter dominated point corresponds to  $(r, m) = (-1, 0)$ . In order to have valid matter era it is required that  $m(r \rightarrow -1) > 0$  and  $-1 < dm/dr(r \rightarrow -1) \leq 0$ . This last condition implies that all the  $m(r)$  trajectories must be between the lines  $m = 0$  and  $m = -r - 1$ . Viable cosmological trajectories for a given  $f(R)$  model in the  $(r, m)$  plane should connect matter dominated point  $P_M = (-1, 0)$  with the de Sitter attractor at the line  $r = -2$  in the region  $0 < m \leq 1$  [40]. The  $\Lambda$ CDM model, for instance, connect the points  $P_M = (-1, 0)$  and  $P_{dS} = (-2, 0)$ . There are also viable trajectories connecting the saddle matter point  $P_M = P_S(m \rightarrow 0)$  with the curvature dominated point  $P_C$  that leads to stable accelerated expansion in the cases  $m' < -1$  and  $(\sqrt{3} - 1)/2 < m < 1$  or  $m' > -1$  and  $m < -(1 + \sqrt{3})/2$  or  $m \geq 1$ .

There is a third type of constraints that are perhaps the most stringent and are related to the local systems where the curvature is much larger than the background curvature. In local systems and also at high curvature (where restrictions from Big Bang nucleosynthesis and the Cosmic Microwave Background appear) the model must be practically indistinguishable from General Relativity, which imply that  $f_{,R}$  should be very close to 1 from below and  $f_{,R}$ , i.e.  $f(R)/R \rightarrow 1$  and  $f_{,R} \rightarrow 1$  as  $R \rightarrow \infty$ .

### Local Gravity Constraints.

To estimate local constraints we appeal to the concept of effective mass for modified gravity that appears from the scalar degree of freedom associated with  $f_{,R}$

$$M^2 = \frac{R}{3} \left( \frac{f_{,R}}{Rf_{,RR}} - 1 \right) = \frac{R}{3m} (1 - m), \quad (2.28)$$

which under the condition  $m \ll 1$ , can be reduced to

$$M^2 \simeq \frac{R}{3m} \simeq \frac{1}{3f_{,RR}}. \quad (2.29)$$

The local gravity constraints are satisfied if  $M\ell \gg 1$ , where  $\ell$  is the typical scale at which the gravity is measured. From (2.29) this constraint can be expressed in terms of  $m$  as

$$m(R_s) \ll \ell^2 R_s, \quad (2.30)$$

where  $R_s$  is the curvature of the local structure, and we assumed  $f_{R_s} \simeq 1$ . To make a numerical estimate we can use the approximation  $R \sim H^2 \sim 8\pi G\rho$ , which applied to the current universe ( $R_0, \rho_0$ ) and to the local structure ( $R_s, \rho_s$ ), allows to write  $R_s \sim H_0^2 \rho_s / \rho_0$  and the above constraint becomes [45]

$$m(R_s) \ll \frac{\rho_s}{\rho_0} \left( \frac{\ell}{H_0^{-1}} \right)^2. \quad (2.31)$$

For the solar system with  $\rho_s \sim 10^{-23} \text{ gr/cm}^3$  and  $\ell \sim 10^{13} \text{ cm}$  one finds that  $m \ll 10^{-24}$ , where we used  $H_0^{-1} \sim 10^{28} \text{ cm}$ .



### 3 The models

We consider a modification to the Einstein gravity with the model

$$f(R) = R - \lambda\mu^2 e^{-\left(\frac{\mu^2}{R}\right)^\eta} \quad (3.1)$$

where  $\mu^2$  is a scale parameter and  $\lambda$  and  $\eta$  are real positive, that will be restricted so that viable the cosmological scenarios take place. This model satisfies the asymptotic behavior

$$\lim_{R \rightarrow \infty} f(R) = R - \lambda\mu^2, \quad \lim_{R \rightarrow 0} f(R) = 0. \quad (3.2)$$

where the first limit leads to consistency with  $\Lambda$ CDM at high redshift, and the limit  $R \rightarrow 0$  leads to disappearing of the cosmological constant and asymptotical flat spacetime, allowing the possibility of pure geometrical explanation of the dark energy problem. The correction to the Einstein gravity is given in the form of convergent series of negative powers of curvature. Negative powers of curvature may appear from some compactification of string/ $M$ -theory as was shown in [16]. However, it is known that curvature corrections of the form  $R^{-n}$ ,  $n > 0$  can accelerate the expansion but lead to non-standard evolution of matter era and are unstable under matter perturbations, among other problems [51]. As we show bellow, when we consider negative powers of  $R$  in the form of convergent series as given in (3.1), then the model not only pass all the consistent restrictions, but also leads to appropriate matter and dark energy dominance eras. From (3.1) follows that the limiting case of  $\Lambda$ CDM can be reached not only at high curvature but also at  $\eta \rightarrow 0$  with cosmological constant  $2\Lambda \rightarrow e^{-1}\mu^2$ .

To check the stability conditions we analyze the derivatives of  $f(R)$ . Taking the first derivative one finds

$$f_{,R} = 1 - \eta\lambda \left(\frac{\mu^2}{R}\right)^{1+\eta} e^{-\left(\frac{\mu^2}{R}\right)^\eta}. \quad (3.3)$$

For  $R > \mu^2$  the condition  $f_{,R} > 0$  can be easily satisfied under the assumption  $\eta\lambda < 1$  and at the limit  $R \rightarrow 0$  the inequality is preserved by the fact that the exponential function decays faster than the power in (3.3). More precisely, since the exponential

function in (3.3) is always less than 1, the condition  $f_{,R} < 1$  can be reduced to

$$\frac{R}{\mu^2} > (\eta\lambda)^{\frac{1}{1+\eta}}. \quad (3.4)$$

The second stability condition involves the second derivative that is given by

$$f_{,RR} = \frac{\eta}{\mu^2} \left(\frac{\mu^2}{R}\right)^{2+\eta} \left(1 + \eta - \eta \left(\frac{\mu^2}{R}\right)^\eta\right). \quad (3.5)$$

Then the condition  $f_{,RR} > 0$  is satisfied if

$$1 + \eta - \eta \left(\frac{\mu^2}{R}\right)^\eta > 0,$$

which is clearly satisfied if  $0 < \eta < 1$  and  $R/\mu^2 > 1$  but admits the fraction  $R/\mu^2$  starting from

$$\frac{R}{\mu^2} > \left(\frac{\eta}{1+\eta}\right)^{1/\eta} \quad (3.6)$$

which can be extremely small for  $\eta \ll 1$ , so that the lower bound on  $R$  can be made as small as necessary, complying with all other conditions. Then the stability conditions  $f_{,R} > 0$  and  $f_{,RR} > 0$  are met if  $0 < \eta < 1$ ,  $\eta\lambda < 1$  and  $R$  satisfies the restriction (3.6).

To check the cosmological viability of this model we analyze the parameters  $m$  and  $r$  to prove the existence of saddle matter era, i.e.  $m(r \rightarrow -1^-) \rightarrow 0^+$  and  $-1 < m'(r \rightarrow -1^-) \leq 0$ . From (2.16) and (2.17) we find the following expressions for  $m$  and  $r$

$$m = \frac{\eta\lambda \left(\frac{\mu^2}{R}\right)^{1+\eta} \left[1 + \eta - \eta \left(\frac{\mu^2}{R}\right)^\eta\right]}{e^{\left(\frac{\mu^2}{R}\right)^\eta} - \eta\lambda \left(\frac{\mu^2}{R}\right)^{1+\eta}}, \quad (3.7)$$

$$r = -\frac{\frac{R}{\mu^2} e^{\left(\frac{\mu^2}{R}\right)^\eta} - \eta\lambda \left(\frac{\mu^2}{R}\right)^\eta}{\frac{R}{\mu^2} e^{\left(\frac{\mu^2}{R}\right)^\eta} - \lambda}. \quad (3.8)$$

Using the parameter  $\lambda$  to fix the de Sitter solution  $r = -2$  at  $R = R_{dS}$  we find

$$\lambda = \frac{y_{dS} e^{\left(\frac{1}{y_{dS}}\right)^\eta}}{2 - \eta \left(\frac{1}{y_{dS}}\right)^\eta}, \quad (3.9)$$

where  $y_{ds}$  is defined by  $y_{ds} = R_{ds}/\mu^2$ . Replacing  $\lambda$  in (2.16) and (2.17) and defining the variable  $y = R/\mu^2$  we find

$$m = \frac{\eta y_{ds} e^{\left(\frac{1}{y_{ds}}\right)^\eta} (1 + \eta - \eta y^{-\eta})}{e^{\left(\frac{1}{y}\right)^\eta} y^{\eta+1} (2 - \eta y_{ds}^{-\eta}) - \eta y_{ds} e^{\left(\frac{1}{y_{ds}}\right)^\eta}}, \quad (3.10)$$

$$r = \frac{\eta y_{ds} e^{\left(\frac{1}{y_{ds}}\right)^\eta} - e^{\left(\frac{1}{y}\right)^\eta} y^{\eta+1} (2 - \eta y_{ds}^{-\eta})}{e^{\left(\frac{1}{y}\right)^\eta} y^{\eta+1} (2 - \eta y_{ds}^{-\eta}) - y_{ds} e^{\left(\frac{1}{y_{ds}}\right)^\eta} y^\eta}. \quad (3.11)$$

The condition of stability at de Sitter point, i.e.  $0 < m(r = -2) \leq 1$ , leads to the following restriction on  $y_{ds}$

$$y_{ds} \geq \left( \frac{2\eta}{3 + \eta - \sqrt{1 + 6\eta + \eta^2}} \right)^{1/\eta}, \quad or \quad (3.12)$$

$$\left( \frac{2\eta}{3 + \eta + \sqrt{1 + 6\eta + \eta^2}} \right)^{1/\eta} \leq y_{ds} < \left( \frac{\eta}{1 + \eta} \right)^{1/\eta} \quad (3.13)$$

For  $\eta \ll 1$  this means that  $y_{ds}$  is practically unrestricted. Fig. 1 shows some trajectories for viable cosmologies in the  $(r, m)$ -plane that connect the matter-dominated saddle point  $P_M$  with the future de Sitter attractor at the line  $r = -2$  with  $0 < m < 1$ . The cosmic evolution of the main density parameters  $\Omega_m$ ,  $\Omega_{DE}$  and  $\Omega_r$  can be obtained from the solution of the dynamical system (2.11)-(2.15) with appropriate initial conditions. Since there is no explicit function for  $m(r)$ , we resort to a polynomial fit to the paths depicted in Fig.1. Taking, for instance, the trajectory with  $\mu = 0.001$ , the numerical fit gives the following approximate function of the dynamical variables  $y[t]$  and  $z[t]$  ( $t = -\ln(1 + z)$ )

$$m = c_0 + c_1 \sqrt{-\frac{z[t]}{y[t]}} + c_2 \frac{z[t]}{y[t]} \quad (3.14)$$

with

$$c_0 = -0.0037076, \quad c_1 = 0.0055066, \quad c_2 = 0.0017984$$

In Fig. 2 we show the evolution of the main density parameters for this case. Any of the trajectories depicted in Fig. 1 leads similar results. The corresponding evolution

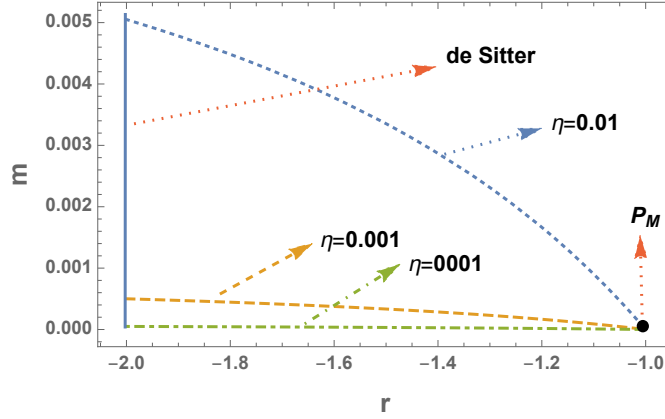


Figure 1: Trajectories in the  $(r, m)$ -plane for three scenarios with  $\eta = 0.01$ ,  $\eta = 0.001$ ,  $\eta = 0.0001$  and  $y_{dS} = 1$ . All trajectories connect the matter dominated saddle point  $P_M$  with the late time de Sitter attractor  $P_{dS}$  at  $r = -2$  with  $0 < m < 1$ .

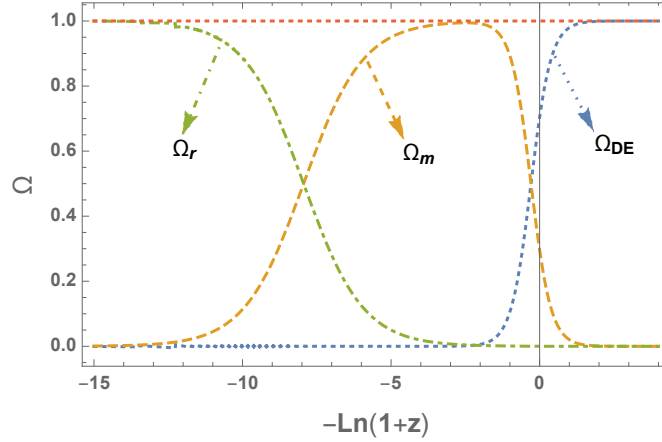


Figure 2: The cosmic evolution of the density parameters for matter, radiation and dark energy for the model (3.1). In this example we take the path of Fig. 1 for  $\eta = 0.001$  and  $y_{dS} = 1$ , using the numerical fit for  $m(r)$  given by the Eq. (3.14), with initial conditions  $x(-5) = 0$ ,  $y(-5) = -0.5$ ,  $z(-5) = 0.500001$  and  $w(-5) = 0.05$ . The behavior is very consistent with the current cosmic observations on the evolution of density parameters. At  $z = 0$ , their approximate values are  $\Omega_m \simeq 0.3$ ,  $\Omega_{DE} \simeq 0.7$  and  $\Omega_r \simeq 10^{-4}$ .

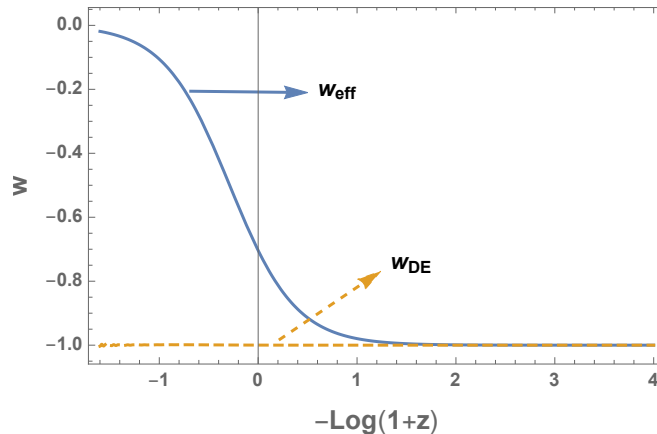


Figure 3: The effective equation of state  $w_{eff}$  and the equation of state associated with the geometric dark energy  $w_{DE}$  for the cosmological evolution of the density parameters described in Fig. 2, corresponding to  $\eta = 0.001$ ,  $y_{ds} = 1$ . The initial conditions lead to a scenario very close to the  $\Lambda$ CDM model.

of the effective and (geometry) dark energy equations of state for this numerical sample is shown in Fig. 3, where the closeness with the  $\Lambda$ CDM model is also evident.

So far we have successfully verified stability conditions and cosmological constraints, but the next more stringent are the local gravity constraints. First we note from (3.9) that for  $\eta \ll 1$  the following relationship takes place

$$\lambda \simeq \frac{e}{2} y_{ds} \quad (3.15)$$

and as  $\eta$  becomes smaller the above relation approaches the equality. This is a consequence of defining the constant  $\lambda$  by fixing the de Sitter curvature at some value  $R_{ds}$ . Taking into account that  $y_{ds} = R_{ds}/\mu^2$ , then the condition  $r = -2$  reflected in (3.9) or (3.15) only determines the ratio  $R_{ds}/\mu^2$ , but two important conditions remain: the product  $\lambda\mu^2$  should be very close, at current epoch, to the expected value of the cosmological constant ( $\Lambda$ ), but also having fixed this value we also need to meet the stringent local gravity constraints. Assuming  $\eta \ll 1$  (starting from  $\eta \sim 10^{-2}$ ), leads for the current epoch to

$$\lambda\mu^2 e^{-\left(\frac{\mu^2}{R_0}\right)^\eta} \sim e^{-1}\lambda\mu^2 \sim \frac{1}{2}y_{ds}\mu^2 = \frac{1}{2}R_{ds} \quad (3.16)$$

On the other hand, from the Friedman equation with cosmological constant follows

$$H^2 = \frac{\kappa^2}{3} \left( \rho_m + \frac{\Lambda}{\kappa^2} \right) = H_0^2 (\Omega_m + \Omega_\Lambda). \quad (3.17)$$

where

$$\Omega_m = \frac{\kappa^2 \rho_{m0}}{3H_0^2} a^{-3}, \quad \Omega_\Lambda = \frac{\Lambda}{3H_0^2}.$$

From Eq. (3.1) we can read

$$\Lambda \approx \Lambda(R \rightarrow \infty) = \frac{1}{2} \lambda \mu^2. \quad (3.18)$$

Then for current epoch the Friedmann equation leads to the known restriction  $1 = \Omega_{m0} + \Omega_\Lambda$ , where  $\Omega_\Lambda \approx 0.7$ . Taking (3.16) and (3.18) into account gives the following result

$$\Omega_\Lambda = \frac{1}{12} \frac{R_{ds}}{H_0^2} = \frac{R_{ds}}{R_0} \approx 0.7. \quad (3.19)$$

Having found the de Sitter curvature  $R_{ds}$  in terms of the current scalar curvature  $R_0$ , we can define the mass scale  $\mu$  by assigning a value to  $y_s$ . Taking the simplest value  $y_s = 1$  we find

$$R_{ds} = \mu^2 \approx 0.7 R_0, \quad \Rightarrow \quad \mu^2 \approx 8.4 H_0^2 \quad (3.20)$$

where  $H_0 \simeq 10^{-33} ev$ . The scale  $\mu$  can be changed without affecting the physical results, it only redefines the de Sitter parameter  $y_{ds}$ . If we set, for instance,  $\mu^2 = H_0^2$ , then  $y_{ds} = 8.4$ .

On the other hand the local gravity constraints can be addressed using the representation for  $m$  given by (3.10). Considering, for instance, the solar system one has  $y_s = R_s/\mu^2$ , where  $R_s \simeq 10^6 H_0^2$  is the curvature for the solar system. As discussed before, the solar system constraints demand  $m \ll 10^{-24}$ . For the parameters  $\eta$  and  $y_{ds}$  as used in Fig.1, we find that if we assume  $y_{ds} = 1$ , then  $y_s \simeq 1.2 \times 10^5$  and

$$\begin{aligned} \eta = 0.01 & \Rightarrow m \simeq 4.2 \times 10^{-8} \\ \eta = 0.001, & \Rightarrow m \simeq 4.2 \times 10^{-9} \\ \eta = 0.0001, & \Rightarrow m \simeq 4.2 \times 10^{-10} \\ \eta = 10^{-18} & \Rightarrow m \simeq 4.2 \times 10^{-24} \\ \eta = 10^{-20} & \Rightarrow m \simeq 5 \times 10^{-26} \end{aligned}$$

Note that although the first three  $\eta$ , corresponding to the trajectories in Fig. 1, satisfy cosmological restrictions, the corresponding values for  $m$  are not small enough to satisfy local gravity constraints. Local constraints begin to be satisfied starting from  $\eta < 10^{-18}$ , making the models cosmologically very close to  $\Lambda$ CDM.

Compared to the Hu-Sawicki (HS) model [44], the present model depends on three parameters ( $\eta, \mu, \lambda$ ) while the HS depends on four ( $m, c_1, c_2, n$ ). In fact, numerical analysis shows that the above numerical results can be obtained from the Hu-Sawicki model by setting  $c_2$  to a suitable value and fixing the de Sitter curvature with  $c_1$  as follows

$$c_1 = \frac{y_{ds}^{1-n} (1 + c_2 y_{ds}^n)^2}{2 - n + 2c_2 y_{ds}^n}, \quad (3.21)$$

where  $n$  and  $y_{ds}$  take the same values used for  $\eta$  and  $y_{ds}$  in the present numerical analysis and  $c_2 = 10^2$ . Note that at the limit  $n \ll 1$  it follows

$$c_1 \simeq \frac{1}{2} y_{ds} (1 + c_2), \quad (3.22)$$

and if additionally  $c_2 \gg 1$ , then

$$\frac{c_1}{c_2} \simeq \frac{1}{2} y_{ds} \left( 1 + \frac{1}{c_2} \right) \simeq \frac{1}{2} y_{ds}, \quad (3.23)$$

which is  $e^{-1}$  times (3.15). Taking for instance  $n = 10^{-3}$  and  $y_{ds} = 1$ , in the Hu-Sawicki model in order to comply with the local gravity constraints, the parameter  $c_2$  must take the value  $c_2 = 10^{16}$ , while for the present model requires  $\eta = 10^{-18}$ . This makes  $c_1/c_2^2 \simeq 5 \times 10^{-17}$  as required by the Hu-Sawicki model to satisfy cosmological and local tests. So, the additional parameter  $c_2$  in the HS model [44] does the job of smaller  $\eta$  ( $< 10^{-18}$ ) in the model (3.1). However under the fact that  $\eta \ll 1$ , the model can not be expanded in powers of  $(\mu^2/R)^\eta$ , retaining only few powers, since the series converges very slowly, so it can not be reduced to HS model.

#### Four Parameter Model.

By adding one more parameter to the model (3.1) we can obtain a new model that offers more possibilities

$$f(R) = R - \lambda \mu^2 e^{-\lambda_1 \left( \frac{\mu^2}{R} \right)^\eta} \quad (3.24)$$

where  $\lambda > 0$ ,  $\lambda_1$ ,  $\eta > 0$ . This model has the same asymptotic limits (3.2) for the model (3.1) and additionally the  $\Lambda$ CDM limit can also be reached at  $\lambda_1 \rightarrow 0$ .

The stability condition  $f_{,R} > 0$  leads to

$$\frac{\mu^2}{R} < \left( \frac{1}{\eta\lambda\lambda_1} \right)^{1/(\eta+1)} \quad (3.25)$$

and  $f_{,RR} > 0$  leads to

$$\frac{\mu^2}{R} < \left( \frac{\eta+1}{\eta\lambda_1} \right)^{1/\eta}. \quad (3.26)$$

If  $\eta\lambda_1 < 1$ ,  $\eta\lambda\lambda_1 < 1$ , then both inequalities are always satisfied as long as  $\mu^2 < R$ . It can be shown that the simultaneous fulfillment of both inequalities takes place for a wide spectrum of parameter values. One can for example define a critical value for  $\lambda$  such that the r.h.s of (3.25) and (3.26) are equal, which takes place for

$$\lambda_c = \frac{1}{\eta+1} \left( \frac{\eta\lambda_1}{\eta+1} \right)^{1/\eta}, \quad (3.27)$$

then if  $\lambda < \lambda_c$ , the stability conditions  $f_{,R} > 0$  and  $f_{,RR} > 0$  are satisfied if (3.26) takes place (i.e.  $f_{,RR} > 0$ ) and in case  $\lambda > \lambda_c$  both stability conditions are satisfied if (3.25) takes place (i.e.  $f_{,R} > 0$ ). This correction the Einstein term can be expanded in powers in the case  $\eta < 1$  and  $\lambda_1 \ll 1$ , since in this case the series converges rapidly. The expansion can also be performed in the case  $\eta > 1$ ,  $\mu^2 < R$  and  $\lambda_1 < 1$  (in fact  $\lambda_1$  can be greater than 1 depending on how big is  $\eta$ )

$$f(R) \approx R - \lambda\mu^2 \left( 1 - \lambda_1 \left( \frac{\mu^2}{R} \right)^\eta \right). \quad (3.28)$$

This expansion is the same as that presented by the HG and Starobinsky [67] models. In fact, numerical analysis shows the same results for the model (3.24) and the HS model with a suitable choice of parameter values.

One important difference with the HS model is that in the HS  $f_{,R}$  diverges in the asymptotic limit ( $R \rightarrow 0$ ) for  $n < 1/2$  and can eventually change the sign, while in the model (3.24) we find that  $\lim_{R \rightarrow 0} f_{,R} = 0$  for any  $\eta > 0$ . The second derivative  $f_{,RR}$  in the HS model also diverges for  $n < 2$  and in general, for the HS model, the  $k$ -th derivative  $|f^k(R)| \rightarrow \infty$  at  $R \rightarrow 0$  for  $n < k$ . For model (3.24) all high derivatives,



like the first derivative, meet the limit  $\lim_{R \rightarrow 0} f_{,RR}, f_{,RRR}, \dots = 0$  for any  $\eta > 0$ . Note also that apart from the common  $\Lambda$ CDM limit at  $R \rightarrow \infty$  in both models, the exact  $\Lambda$ CDM limit in model (3.24) can also be obtained at  $\lambda_1 \rightarrow 0$  (independent of  $R$ ) while in the HS it requires  $R \gg m^2$  and  $c_1/c_2^2 \rightarrow 0$ .

Using  $\lambda$  to fix the de Sitter curvature from  $r = -2$  at  $R = R_{ds}$  we find ( $R_{ds} = \mu^2 y_{ds}$ )

$$\lambda = \frac{y_{ds} e^{\lambda_1 \left(\frac{1}{y_{ds}}\right)^\eta}}{2 - \eta \lambda_1 \left(\frac{1}{y_{ds}}\right)^\eta}. \quad (3.29)$$

Under the condition  $\lambda_1 \ll 1$  this expression can be kept very close to the limit

$$\lambda \simeq \frac{1}{2} y_{ds}, \quad (3.30)$$

which is the same limit (3.23) of the HS model. All results from (3.16) to (3.20) are also valid for the model (3.24) for  $\lambda_1 \ll 1$ .

Replacing  $\lambda$  in (2.16) and (2.17) we find ( $R = \mu^2 y$ )

$$m = \frac{\eta \lambda_1 y_{ds} e^{\lambda_1 \left(\frac{1}{y_{ds}}\right)^\eta} (1 + \eta - \eta \lambda_1 y^{-\eta})}{e^{\lambda_1 \left(\frac{1}{y}\right)^\eta} y^{\eta+1} (2 - \eta \lambda_1 y_{ds}^{-\eta}) - \eta \lambda_1 y_{ds} e^{\lambda_1 \left(\frac{1}{y_{ds}}\right)^\eta}}, \quad (3.31)$$

$$r = \frac{\eta \lambda_1 y_{ds} e^{\lambda_1 \left(\frac{1}{y_{ds}}\right)^\eta} - e^{\lambda_1 \left(\frac{1}{y}\right)^\eta} y^{\eta+1} (2 - \eta \lambda_1 y_{ds}^{-\eta})}{e^{\lambda_1 \left(\frac{1}{y}\right)^\eta} y^{\eta+1} (2 - \eta \lambda_1 y_{ds}^{-\eta}) - y_{ds} e^{\lambda_1 \left(\frac{1}{y_{ds}}\right)^\eta} y^\eta}. \quad (3.32)$$

From the condition of stability at de Sitter point, i.e.  $0 < m(r = -2) \leq 1$ , and assuming  $\eta > 0$ ,  $\lambda_1 > 0$ , we find the following restriction on  $y_{ds}$

$$y_{ds} \geq \left( \frac{2\eta\lambda_1}{3 + \eta - \sqrt{1 + 6\eta + \eta^2}} \right)^{1/\eta}, \quad or \quad (3.33)$$

$$\left( \frac{2\eta\lambda_1}{3 + \eta + \sqrt{1 + 6\eta + \eta^2}} \right)^{1/\eta} \leq y_{ds} < \left( \frac{\eta\lambda_1}{1 + \eta} \right)^{1/\eta} \quad (3.34)$$

which leaves  $y_{ds}$  practically unrestricted for  $\eta > 0$ , given that  $\lambda_1$  is a free parameter. In Fig. 4 we show trajectories for the case  $\eta < 1$  in the  $(r - m)$ -plane for the model (3.24) which are contrasted with the similar trajectories for the HS model. Although all the curves in Fig.1 describe cosmologically viable scenarios, they fail to meet local

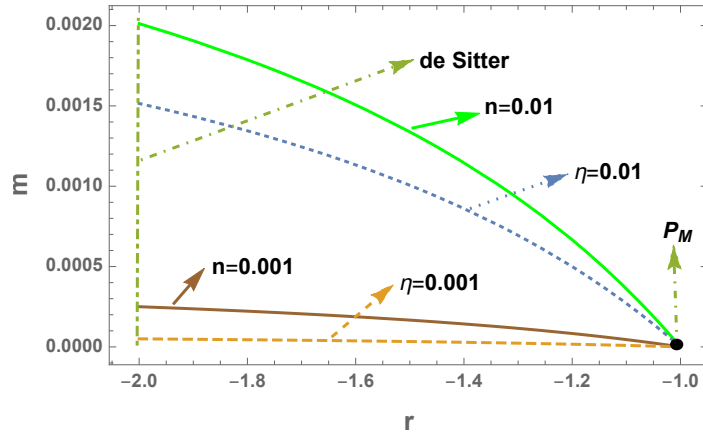


Figure 4: Viable cosmological trajectories that connect the matter-dominated saddle critical point  $P_M$  with the late-time de Sitter attractor at  $r = -2$  with  $0 < m < 1$ . The dashed line curves for the model (3.24) correspond to  $(\eta = 0.01, \lambda_1 = 0.3)$  (dotted) and  $(\eta = 0.001, \lambda_1 = 0.1)$  (dashed) and continuous lines for the HS model correspond to  $(n = 0.01, c_2 = 1.5)$  (green) and  $(n = 0.001, c_2 = 1)$  (brown), where in all cases  $y_{ds} = 1$ . The models can match each other with high accuracy, but the intention of the graphic is to highlight each model.

gravity constraints for the proposed values of the parameters. As shown in table below, the model (3.1) needs much smaller  $\lambda_1$  while the HS model demands much larger  $c_2$  in inverse proportion to  $\lambda_1$ , in order to satisfy local gravity constraints.

$\eta$	$\lambda_1$	$m(y_s)$	$n$	$c_2$	$m^{(HS)}(y_s)$
$10^{-2}$	0.3	$1.1 \times 10^{-8}$	$10^{-2}$	1.5	$1.6 \times 10^{-8}$
$10^{-3}$	0.1	$4.1 \times 10^{-10}$	$10^{-3}$	1	$2.1 \times 10^{-9}$
$10^{-2}$	$10^{-16}$	$3.7 \times 10^{-24}$	$10^{-2}$	$10^{16}$	$3.7 \times 10^{-24}$
$10^{-3}$	$10^{-16}$	$4.1 \times 10^{-25}$	$10^{-3}$	$10^{16}$	$4.1 \times 10^{-25}$
$10^{-6}$	$10^{-18}$	$4.2 \times 10^{-30}$	$10^{-6}$	$10^{18}$	$4.2 \times 10^{-30}$

**Table I**

In this table we show some numerical values for the parameter  $m = \frac{Rf_{,RR}}{f_{,R}}$  for the solar system where we have set  $y_{ds} = 1$  for both models which leads to  $\mu^2$ ,  $m^2 \approx 8.4H_0^2$ . This results in  $y_s \approx 1.2 \times 10^5$  for the solar system. The parameter is represented by  $m$  for the model (3.24) and by  $m^{(HS)}$  for the HS model. Then, all restrictions can be accomplished by the model (3.24) for  $\eta < 1$  with suitable choice of  $\lambda_1$ . Here we used the results (3.30) and (3.22) for  $\lambda$  and  $c_1$  respectively, which lead to the same prediction for  $R_{ds}$  obtained in (3.19).

The model (3.24) leads also to interesting results for  $\eta > 1$ . In this case, keeping  $R > \mu^2$ , the expansion (3.28) can be more accurate even if  $\lambda_1 \gtrsim 1$ . In Fig. 5 we show some viable trajectories which are contrasted with those of the HS model. In order to satisfy local gravity constraints, for the typical case of the solar system where  $m \ll 10^{-24}$  ( $y_s \approx 1.2 \times 10^5 H_0$ ), we need larger  $\eta$ ,  $n$  and or suitable choice of  $\lambda_1$  in the model (3.24) or  $c_2$  in the HS model. In table 2 bellow we present some cases

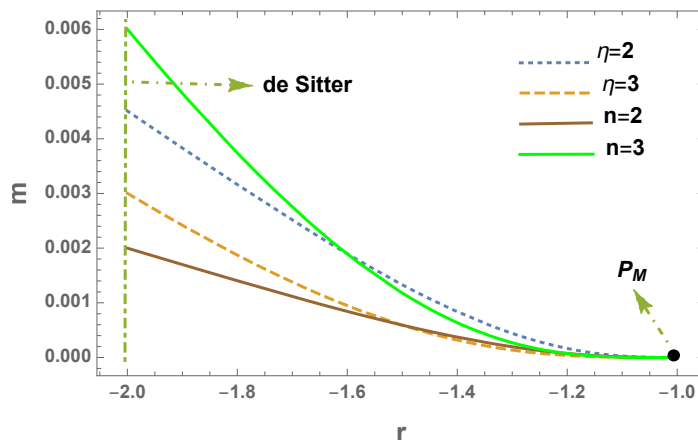


Figure 5: Viable cosmological trajectories for the model (3.24) with  $\eta > 1$ , where dotted line corresponds to  $(\eta = 2, \lambda_1 = 1.5 \times 10^{-5})$  and dashed line to  $(\eta = 3, \lambda_1 = 5 \times 10^{-6})$ . To compare, we plotted trajectories for the HS model corresponding to  $(n = 2, c_2 = 1.5 \times 10^5)$  and  $(n = 3, c_2 = 10^5)$ . In all cases we used  $y_{ds} = 1$ , that corresponds to  $\mu^2 = m^2 \approx 8.4H_0^2$ .

$\eta$	$\lambda_1$	$m(y_s)$	$n$	$c_2$	$m^{(HS)}(y_s)$
2	$1.5 \times 10^{-3}$	$2.6 \times 10^{-18}$	2	$1.5 \times 10^3$	$1.2 \times 10^{-18}$
2	$1.5 \times 10^{-9}$	$2.6 \times 10^{-24}$	2	$1.5 \times 10^9$	$1.1 \times 10^{-24}$
3	$5 \times 10^{-4}$	$1.4 \times 10^{-23}$	3	$10^3$	$2.9 \times 10^{-23}$
3	$5 \times 10^{-5}$	$1.4 \times 10^{-24}$	3	$10^4$	$2.9 \times 10^{-24}$
4	$10^{-5}$	$4 \times 10^{-30}$	4	$10^5$	$4 \times 10^{-30}$

**Table II**

So, the model (3.24) comply with all requirements of viability for a geometrical description of dark energy, giving results for the evolution of density parameters and the equation of state totally consistent with current observations and very close to  $\Lambda$ CDM model, in the two regimes,  $\eta < 1$  and  $\eta > 1$ . Nevertheless the dynamical nature of the above proposed corrections to General Relativity should reveal features that allow to differentiate them from the cosmological constant. According to the study of growth of matter perturbations, in the scale of validity of linear regime

( $10^{-2}Mpc^{-1} \lesssim k \lesssim 0.15Mpc^{-1}$ ) [81, 82, 83, 84], some  $f(R)$  may behave in such a way that can be distinguished from  $\Lambda$ CDM and this effect could be sensitive to near future observations. The transition from GR regime to scalar tensor regime may be established when the effective mass scale  $M$  associated with the  $f(R)$  model (see (2.29)) is comparable to the inverse of the scale length  $\ell = a/k$ , i.e.

$$\ell^2 M^2 \approx 1 \Rightarrow M^2 \simeq \frac{k^2}{a^2}, \Rightarrow m \approx \left(\frac{aH}{k}\right)^2, \quad (3.35)$$

where the last relation follows from (2.29). According to this, in order that a region of size  $\ell$  is not affected by modifications of gravity it must be  $\ell M \gg 1$ , which applied to cosmic scales means that effects of modified gravity can appear at scales smaller than  $M^{-1}$ . If we consider a galaxy cluster with a size  $\ell$  of the order of 10Mpc, then the following relations apply

$$\ell \sim \frac{a}{k} \sim \frac{1}{H} = 10Mpc \approx 3.26 \times 10^7 ly. \quad (3.36)$$

If  $\ell_0$  is the size of the universe, then

$$\ell_0 \sim \frac{a_0}{k_0} \sim \frac{1}{H_0} \approx 1.38 \times 10^{10} ly, \quad (3.37)$$

and

$$\frac{k}{k_0} = \frac{\ell_0}{\ell} \approx 4.2 \times 10^2 \Rightarrow k \approx 420k_0 \approx 420a_0H_0 \quad (3.38)$$

this wave number is near the upper limit of the scale relevant to the galaxy power spectrum as cited above, which is between the validity of the linear regime [82]. Thus, if the transition to scalar-tensor regime occurred in the representative current epoch, then  $m(z \sim 0)$  should satisfy the condition

$$m(z \approx 0) \gtrsim (420)^{-2} \approx 5.6 \times 10^{-6}, \quad (3.39)$$

in order to find deviations from GR at scales  $k \sim 0.1Mpc^{-1}$ . In table III we show values of  $m(z \approx 0)$  for the models (3.1) and (3.24) and considering parameters values that are consistent with local gravity constraints.

$\eta < 1$			$\eta > 1$		
$\eta$	$\lambda_1$	$m(y_0)$	$\eta$	$c_2$	$m(y_0)$
0.01	$10^{-16}$	$3.6 \times 10^{-19}$	2	$1.5 \times 10^{-9}$	$1.6 \times 10^{-9}$
0.001	$10^{-16}$	$3.6 \times 10^{-20}$	3	$5 \times 10^{-5}$	$7.8 \times 10^{-5}$
$10^{-4}$	$10^{-14}$	$3.6 \times 10^{-19}$	4	$10^{-4}$	$1.8 \times 10^{-4}$
$10^{-6}$	$10^{-14}$	$4.1 \times 10^{-21}$	5	$10^{-3}$	$2 \times 10^{-3}$

**Table III**

where using  $\mu^2 \approx 8.4H_0^2$ , the current epoch corresponds to  $y_0 \approx 1.4$ . The same order of magnitude is shown correspondingly by the cases  $n < 1$  and  $n > 1$  in the HS model. These results show that the differences with  $\Lambda$ CDM are practically undetectable for models with  $\eta < 1$  (at least at the level of validity of linear approximation in the growth of matter perturbations), while models with  $\eta > 1$  can lead to measurable differences with  $\Lambda$ CDM, that could be detected with the next improvement in the precision of observations.

## 4 Discussion

The introduction of a kind of exponential damping in the correction to GR (3.1), (3.24) gives promising results in the construction of viable DE model in the context of modified gravity. The function  $f(R)$  satisfies the condition  $f(0) = 0$ , which implies the absence of cosmological constant in the flat space-time limit, so that the curvature effect that induces the accelerated expansion is unrelated to quantum vacuum energy in flat space-time. The model (3.1) satisfies the conditions of stability during the whole cosmological evolution from matter era to future de Sitter attractor, and passes local and cosmological viability tests in the regime  $\eta \ll 1$ , while the model (3.24) satisfies all above conditions in the regimes  $0 < \eta < 1$  and  $\eta \geq 1$ . Both models lead to a consistent with observations evolution of the main cosmological parameters, with  $w_{eff}$  showing the transition to the accelerated phase at the currently observed  $z_t \sim 0.5$ , and  $w_{DE} \simeq -1$  (numerical example was shown for the case  $\eta = 10^{-3}$ ).

Using the limit of the Friedmann equation with cosmological constant (3.17)-(3.20) it was shown that the models (3.1) and (3.24) predict a de Sitter curvature  $R_{ds} \approx \Omega_\Lambda R_0$ , where  $R_0$  is the scalar curvature at current epoch. The model was compared to the HS model and it was shown that, with a suitable choice of parameters, the model (3.24) leads to the same results as the HS model. However, there are differences with the HS model. Apart from the simplicity of the correction to GR, the model (3.24) contains the  $\Lambda$ CDM (apart from the limits  $R \rightarrow \infty$  and  $\mu \rightarrow zero$ ) in the limit  $\lambda_1 \rightarrow 0$ , independent of  $R$ , while in HS it must be  $R \gg m^2$  and  $c_1/c_2^2 \rightarrow 0$ . An advantage of the model (3.24) compared to HS is in the asymptotic behavior of derivatives: in the HS model  $f_{,R}$  diverges in the asymptotic limit ( $R \rightarrow 0$ ) for  $n < 1/2$  and can eventually change the sign, while in the model (3.24) we find that  $\lim_{R \rightarrow 0} f_{,R} = 0$  for any  $\eta > 0$ . The second derivative  $f_{,RR}$  in HS also diverges for  $n < 2$  and in general, for the HS model, the  $k$ -th derivative  $|f^k(R)| \rightarrow \infty$  at  $R \rightarrow 0$  for  $n < k$ . For the model (3.24) all high derivatives, just like the first, satisfy the limit  $\lim_{R \rightarrow 0} f_{,RR}, f_{,RRR}, \dots = 0$  for any  $\eta > 0$ .

On the other hand, from tables I and II it becomes clear that in order to satisfy the more stringent local gravity tests the models should be very close to  $\Lambda$ CDM, but it is also observed from table III that the deviation parameter  $m(r)$  for  $\eta > 1$  grows faster from the matter era to the current epoch than in models with  $\eta < 1$ . This increase in  $m(r)$ , by several orders of magnitude, may be sensitive to the transition from GR regime to scalar tensor regime (at scales of validity of linear regime  $10^{-2} Mpc^{-1} \lesssim k \lesssim 0.15 Mpc^{-1}$  in the growth of matter perturbations) and opens the possibility of detecting differences with  $\Lambda$ CDM in recent times with the improvement of observational techniques in the near future.

## Acknowledgments

This work was supported by Universidad del Valle under project CI 71187.

## References

- [1] G. W. Horndeski, *Int. J. Theor. Phys.* **10**, 363 (1974).
- [2] A. Nicolis, R. Rattazzi, E. Trincherini, *Phys. Rev. D* **79**, 064036 (2009); arXiv:0811.2197 [hep-th]
- [3] C. Deffayet, G. Esposito-Farese, A. Vikman, *Phys. Rev. D* **79**, 084003 (2009), arXiv:0901.1314 [hep-th]
- [4] E. J. Copeland, M. Sami and S. Tsujikawa, *Int. J. Mod. Phys. D* **15** 1753-1936 (2006), arXiv:hep-th/0603057
- [5] V. Sahni, *Lect. Notes Phys.* **653**, 141-180 (2004), arXiv:astro-ph/0403324v3
- [6] T. Padmanabhan, *Phys. Rept.* **380**, 235 (2003), [hep-th/0212290].
- [7] K. Bamba, S. Capozziello, S. Nojiri, S. D. Odintsov, *Astrophys. and Space Sci.* **342**, 155 (2012); arXiv:1205.3421 [gr-qc]
- [8] S. Nojiri and S. D. Odintsov, *Int. J. Geom. Meth. Mod. Phys.* **4**, 115 (2007) [arXiv:hep-th/0601213].
- [9] T. P. Sotiriou, V. Faraoni, *Rev. Mod. Phys.* **82**, 451 (2010); arXiv:0805.1726 [gr-qc].
- [10] S. Tsujikawa, *Lect. Notes Phys.* **800**, 99 (2010); arXiv:1101.0191 [gr-qc]
- [11] S. Nojiri, S.D. Odintsov, *Int. J. Geom. Meth. Mod. Phys.* **11**, 1460006 (2014); [arXiv:1306.4426 [gr-qc]].
- [12] S. Nojiri, S. D. Odintsov, *Phys. Rept.* **505** (2011) 59-144; arXiv:1011.0544 [gr-qc]
- [13] S. Nojiri, S. D. Odintsov, V. K. Oikonomou, *Phys. Rept.* **692** (2017) 1-104; arXiv:1705.11098 [gr-qc]
- [14] S. Capozziello, *Int. J. Mod. Phys. D* **11**, 483 (2002); gr-qc/0201033



- [15] S. Capozziello, S. Carloni, A. Troisi, *Recent Res. Dev. Astron. Astrophys* **1**, 625 (2003); astro-ph/0303041
- [16] S. Nojiri and S.D. Odintsov, *Phys. Lett. B* **576**, 5 (2003); hep-th/0307071
- [17] S. Nojiri and S. D. Odintsov, *Phys. Rev. D* **68**, 123512 (2003); arXiv:hep-th/0307288.
- [18] S. M. Carroll, V. Duvvuri, M. Trodden and M. S. Turner, *Phys. Rev. D* **70**, 043528 (2004); arXiv:astro-ph/0306438
- [19] S. Nojiri and S. D. Odintsov, *Gen. Rel. Grav.* **36**, 1765 (2004), hep-th/0308176.
- [20] M. C. B. Abdalla, S. Nojiri, and S. D. Odintsov, *Class. Quant. Grav.* **22**, L35 (2005); hep-th/0409177.
- [21] G. Cognola, E. Elizalde, S. Nojiri, S. D. Odintsov, and S. Zerbini, *JCAP* **0502**, 010 (2005); hep-th/0501096.
- [22] S. Capozziello, V. F. Cardone, and A. Troisi, *Phys. Rev. D* **71**, 043503 (2005); astro-ph/0501426
- [23] G. Allemandi, A. Borowiec, M. Francaviglia, and S. D. Odintsov, *Phys. Rev. D* **72**, 063505 (2005); gr-qc/0504057
- [24] T. Koivisto and H. Kurki-Suonio, *Class. Quant. Grav.* **23**, 2355 (2006); astro-ph/0509422.
- [25] M. Sami, A. Toporensky, P. V. Tretjakov, and S. Tsujikawa, *Phys. Lett. B* **619**, 193 (2005), hep-th/0504154.
- [26] T. Clifton and J. D. Barrow, *Phys. Rev. D* **72**, 103005 (2005), gr-qc/0509059.
- [27] V. Faraoni, *Phys. Rev. D* **72**, 124005 (2005); gr-qc/0511094.
- [28] I. Brevik, *Int. J. Mod. Phys. D* **15**, 767 (2006); gr-qc/0601100
- [29] T. Koivisto, *Phys. Rev. D* **73**, 083517 (2006), astro-ph/0602031.

- [30] T. P. Sotiriou, *Class. Quant. Grav.* **23**, 5117 (2006), gr-qc/0604028.
- [31] S. Capozziello, S. Nojiri, S. D. Odintsov, and A. Troisi, *Phys. Lett. B* **639**, 135 (2006); astro-ph/0604431
- [32] A. de la Cruz-Dombriz and A. Dobado, *Phys. Rev. D* **74**, 087501 (2006); gr-qc/0607118.
- [33] S. Nojiri and S. D. Odintsov, *Phys. Rev. D* **74**, 086005 (2006); hep-th/0608008
- [34] A. W. Brookfield, C. Van de Bruck, and L. M. H. Hall, *Phys. Rev. D* **74**, 064028 (2006); hep-th/0608015.
- [35] S. Nojiri and S. D. Odintsov (2006), *J. Phys. A* **40**, 6725 (2007); hep-th/0610164
- [36] V. Faraoni, *Phys. Rev. D* **74**, 104017 (2006), astro-ph/0610734.
- [37] Y.-S. Song, W. Hu, and I. Sawicki, *Phys. Rev. D* **75**, 044004 (2007), astro-ph/0610532.
- [38] R. Bean, D. Bernat, L. Pogosian, A. Silvestri, M. Trodden, *Phys. Rev. D* **75**, 064020 (2007), astro-ph/0611321.
- [39] G. J. Olmo, *Phys. Rev. D* **75**, 023511 (2007); gr-qc/0612047.
- [40] L. Amendola, R. Gannouji, D. Polarski and S. Tsujikawa, *Phys. Rev. D* **75**, 083504 (2007); [arXiv:gr-qc/0612180].
- [41] B. Li and J. D. Barrow, *Phys. Rev. D* **75**, 084010 (2007); gr-qc/0701111.
- [42] S. Fay, S. Nesseris, and L. Perivolaropoulos, *Phys. Rev. D* **76**, 063504 (2007), gr-qc/0703006.
- [43] V. Faraoni, *Phys. Rev. D* **75**, 067302 (2007), gr-qc/0703044.
- [44] W. Hu and I. Sawicki, *Phys. Rev. D* **76**, 064004 (2007); [arXiv:astro-ph/0705.1158].

- [45] S. Tsujikawa, Phys. Rev. D **77**, 023507 (2008); arXiv:0709.1391 [astro-ph]
- [46] E. Elizalde, S. Nojiri, S. D. Odintsov, L. Sebastiani, S. Zerbini, Phys. Rev. D **83**, 086006 (2011); arXiv:1012.2280
- [47] S. D. Odintsov, V. K. Oikonomou, Nucl. Phys. B **293**, 608 (2017); arXiv:1708.08346
- [48] S. D. Odintsov, D. Saez-Chillon, G. S. Sharov, Eur. Phys. J. C **77**, 862 (2017); arXiv:1709.06800
- [49] S. D. Odintsov, D. Saez-Chillon, G. S. Sharov, Phys. Rev. D **99**, 024003 (2019); arXiv:1807.02163
- [50] A. A. Starobinsky, Phys. Lett. B **91**, 99 (1980).
- [51] A. D. Dolgov and M. Kawasaki, Phys. Lett. B **573**, 1 (2003); [arXiv:astro-ph/0307285].
- [52] L. Amendola, D. Polarski and S. Tsujikawa, Phys. Rev. Lett. **98**, 131302 (2007) [arXiv:astro-ph/0603703].
- [53] S. Nojiri and S. D. Odintsov, Phys. Lett. B **657**, 238 (2007); arXiv: 0707.1941 [hep-th]
- [54] S. Nojiri and S. D. Odintsov, Phys. Rev. D **77**, 026007 (2008); arXiv:0710.1738 [hep-th]
- [55] S. Nojiri and S. D. Odintsov, Phys. Rev. D **77**, 046009 (2008); arXiv:0712.4017 [hep-th]
- [56] S. Nojiri, S. D. Odintsov, M. Sasaki, Phys. Rev. D **71**, 123509 (2005), hep-th/0504052.
- [57] S. Nojiri and S. D. Odintsov, Phys. Lett. B **631** (2005), 1; arXiv:hep-th/0508049.
- [58] S. Nojiri, S. D. Odintsov, O. G. Gorbunova, J. Phys. A **39** (2006), 6627.

- [59] G. Cognola, E. Elizalde, S. Nojiri, S. D. Odintsov and S. Zerbini, Phys. Rev. D **73** (2006), 084007; arXiv:hep-th/0601008
- [60] K. Bamba, S. Nojiri, S.D. Odintsov, JCAP **0810**, 045 (2008); [arXiv:0807.2575 [hep-th]].
- [61] J. D. Barrow, T. Clifton, Class. Quant. Grav. **23**, L1 (2005).
- [62] T. Clifton, J. D. Barrow, Class. Quant. Grav. **23**, 2951 (2006).
- [63] S. Capozziello and A. De Felice, JCAP **0808**, 016 (2008).
- [64] S. Capozziello, A. Stabile, and A. Troisi, Class. Quant. Grav. **24**, 2153 (2007).
- [65] S. Capozziello, A. Stabile, A. Troisi, Class. Quant. Grav., **25**, 085004 (2008)
- [66] J. D. Barrow, S. Cotsakis, Phys. Lett. B **214**, 515 (1988).
- [67] A. A. Starobinsky, JETP Lett. **86**, 157 (2007)
- [68] S. A. Appleby and R. A. Battye, Phys. Lett. **B 654**, 7 (2007); arXiv:0705.3199 [astro-ph]
- [69] S. Nojiri, S. D. Odintsov, Phys. Lett. B **652**, 343 (2007); arXiv:0706.1378 [hep-th]
- [70] G. Cognola, E. Elizalde, S. Nojiri, S.D. Odintsov, L. Sebastiani, S. Zerbini, Phys. Rev. D **77**, 046009 (2008); arXiv:0712.4017 [hep-th].
- [71] E. Elizalde, S. Nojiri, S.D. Odintsov, L. Sebastiani, S. Zerbini, Phys. Rev. D **83**, 086006 (2011); [arXiv:1012.2280 [hep-th]].
- [72] J. C. C. de Souza, V. Faraoni, Class. Quant. Grav. **24**, 3637 (2007); arXiv:0706.1223 [gr-qc]
- [73] G. Leon, E.N. Saridakis, JCAP **1504**, 031 (2015); arXiv:1501.00488 [gr-qc]
- [74] S.D. Odintsov, V.K. Oikonomou, P. V. Tretyakov, Phys. Rev. D **96**, 044022 (2017); arXiv:1707.08661 [gr-qc]

- [75] S.D. Odintsov, V.K. Oikonomou, Phys. Rev. D **96**, 104049 (2017); arXiv:1711.02230 [gr-qc]
- [76] S.D. Odintsov, V.K. Oikonomou, Phys. Rev. D **98**, 024013 (2018); arXiv:1806.07295 [gr-qc]
- [77] S. Capozziello and S. Tsujikawa, Phys. Rev. D **77**, 107501 (2008); arXiv:0712.2268.
- [78] P. Brax, C. van de Bruck, A. Davis, and D. J. Shaw. Phys. Rev. D **78**, 104021 (2008); arXiv:0806.3415.
- [79] L. N. Granda, Eur. Phys. J. C. **80**, 538 (2020); arXiv:2003.09006 [gr-qc]
- [80] L. Granda, Symmetry **12**, 794 (2020);
- [81] E. V. Linder, Phys. Rev. D **72**, 043529 (2005); arXiv:astro-ph/0507263
- [82] W. J. Percival et. al, Astrophys. J. **657**, 645 (2007).
- [83] D. Huterer and E. V. Linder, Phys. Rev. D **75**, 023519 (2007); arXiv:astro-ph/0608681
- [84] S.Tsujikawa, R. Gannouji, B. Moraes, D. Polarski, Phys. Rev. D **80**, 084044 (2009); arXiv:0908.2669 [astro-ph.CO]